Check for updates

Potentially toxic elements and rare earth elements in sandy soils from the Brazilian Cerrado

Vanessa Martins · Ronny Sobreira Barbosa [ID] · Ozeas S Costa Jr ·
Yuri Jacques Agra Bezerra da Silva · Ygor Jacques Agra Bezerra da Silva ·
Julio César Galdino de Sousa · Gabriela Bielefeld Nardoto

Abstract This study aims to determine the concentration of potentially toxic elements (PTEs) and rare earth elements (REEs) in Brazilian sandy soils under the Cerrado at the Parnaíba–São Francisco Basin transition. We also explored the geochemical correlation between these elements and pH, cation exchange capacity (CEC), total organic carbon (TOC), sand, clay, oxides from secondary minerals, and chemical index of alteration for each basin. Mineralogical, physical, and chemical analyses were used to examine PTE and REE geochemistry in six sand soil profiles from the Brazilian Cerrado. The background concentrations of these elements are low, but soils from the Parnaíba Basin have higher concentrations of PTEs than soils from the São Francisco Basin. In soils from the Parnaíba Basin, mainly Al_2O_3 has relevance in the V and Cr geochemistry, as these elements increase with increasing Al_2O_3 content. On the other hand, the REEs have CEC as a soil attribute of higher relevance in the geochemistry of those elements is soils from the Parnaíba Basin, and this relevance divides the TOC, Fe_2O_3, and TiO_2 minerals from the clay fraction. In soils from the São Francisco Basin, the geochemistry of PTEs is possibly associated with kaolinite, especially Cu, V, and Zn. In contrast, the Ba concentration was associated with the presence of feldspar. Unlike soils from the Parnaíba Basin, the REEs do not correlate with the studied soil attributes, except for Ho and Lu. Ho had a positive association with Al_2O_3. Ho and Lu are negatively related to the presence of iron oxides.

Keywords Trace elements · Lanthanides · Background concentration · Geochemistry · Tropical soils · State of Piauí

V. Martins
Technical College of Bom Jesus, High School Level, Federal University of Piauí, Manoel Gracindo Street, km 01, Planalto Horizonte, Bom Jesus, PI 64900-000, Brazil

R. S. Barbosa (✉) · Y. J. A. B. da Silva · J. C. G. de Sousa
Agronomy Undergraduate Course, Federal University of Piauí, Campus Professora Cinobelina Elvas, Manoel Gracindo Street, km 01, Planalto Horizonte, Bom Jesus, PI 64900-000, Brazil
e-mail: ronny.barbosa@ufpi.edu.br

O. S. Costa Jr
The Ohio State University at Mansfield, 1760 University Dr, Mansfield, OH 44906, USA

Y. J. A. B. da Silva
Agronomy Department, Federal Rural University of Pernambuco, Dom Manuel de Medeiros Street, s/n, Dois Irmãos, PE 52171-900, Brazil

G. B. Nardoto
Departament of Ecology, University of Brasília, Asa Norte, Campus Universitário Darcy Ribeiro, Brasília, DF 70910-900, Brazil

Introduction

The Cerrado, one of the world's biodiversity hotspots (Mittermeier et al., 2005), is the second

Springer

largest biome in Brazil, encompassing approximately 2,036,448 km^2, covering more than 20% of the national territory. According to the Food and Agriculture Organization of the United Nations (FAO), it has been extensively used for different purposes, including agriculture (Rótolo et al., 2015). Authors have been reported that at least 80% of the Cerrado face some kind of anthropogenic pressure (Beuchle et al., 2015; Marafon et al., 2020). The climate regime, typical flat topography, and mostly clayey soils have provided prime conditions for intensive agricultural and livestock expansion since 1970 (Silva et al., 2006).

Regardless of the clayey soil's representativity in the Cerrado territory, sandy soils (i.e., sand content higher than 700 g kg^{-1}) are also relevant. This is mainly because agricultural use has been increasing over the years (Rodrigues & Silva, 2020). Sandy soils cover approximately 900 million ha worldwide, with 126 million distributed in South and Central America (Yost & Hartemink, 2019). A representative part of the Brazilian Northeastern Cerrado is embraced by the State of Piauí (approximately 120,000 km^2), distributed between the Parnaíba Basin and the São Francisco Basin (Matos & Felfili, 2010), which is mostly represented by sandy soils (Pfaltzgraff et al., 2010). Given that they have not been frequently used for agriculture worldwide (Yost & Hartemink, 2019), research on such soil types is limited, and their understanding is a global priority for their sustainability.

Several soil attributes have been assessed to achieve this understanding. To highlight the relevance of soil conservation when used in chemical management activities, both potentially toxic elements (PTEs) and rare earth elements (REEs) are emphasized. This emphasis occurs because their occurrence in soils is associated with either pedological or anthropic processes (Bolarinwa & Bute, 2016; Kabata-Pendias, 2011). Efforts to establish scientific advantages in understanding the background of these elements and their geochemistry in Cerrado sandy soils have not been frequent, especially for PTEs. On the other hand, Oliveira et al. (2013) and Pereira et al. (2019) investigated the geochemistry of REEs in Cerrado soils; however, they only covered the topsoil layers. Nevertheless, only the investigations carried out by Oliveira et al.

(2013) and Pereira et al. (2019) considered the relevance of sandy soils. Therefore, the amount of information about PTEs and REEs in sandy soil profiles is insufficient and needs improvement.

Some authors have reported that concentrations of both PTEs and REEs are related to soil parent materials (Kabata-Pendias, 2011; Silva et al., 2018; Silva et al., 2020). Mafic and ultramafic rocks are known as providers of soils with high concentrations of PTEs (Alfaro et al., 2015; Chrysochoou et al., 2016; Gonzalez-Rodriguez & Fernandez-Marcos, 2021) and REEs (Alfaro et al., 2018), whereas sedimentary rocks, except calcareous, generally provide relatively small concentrations of these elements in soils (Nascimento et al., 2018; Silva et al., 2018).

Nevertheless, the PTEs and REEs concentrations may also be associated with weathering due to their interface with soil chemical reactions. For instance, according to Chrysochoou et al. (2016), forms of Cr are controlled by chemical weathering reactions such as oxidation that convert Cr^{3+} to Cr^{6+} after releasing Cr^{3+} into the soil solution due to mineral weathering. The mineral weathering also may be cited as the main responsible for the representative losses of REEs during the soil formation as reported by Laveuf and Cornu (2009).

The geochemistry of PTEs and REEs may be assessed by observing different soil attributes. Hamidpour et al. (2019) report that the dynamic of Zn and Cd may be affected by soil pH, whereas Zhu et al. (2018) and Savignan et al. (2021) highlighted the relevance of pH, $CaCO_3$, and cation exchange capacity (CEC) in the dynamic of PTEs. Mihajlovic and Rinklebe (2018) reveal that soil attributes as clay content and total organic carbon (TOC) may have significant relations with REEs geochemistry, whereas Davranche et al. (2015) report that the CEC is related to REEs due to chelation, which is also associated with the TOC.

Our results are essential to establish both background concentration and the relationship between PTEs and REEs in representative sandy soils from the Brazilian Cerrado of Piauí State. Thus, this study aimed to determine the PTE and REE concentrations in Brazilian sandy soils under the Cerrado at the Parnaíba–São Francisco Basin transition. We also explored the geochemical correlation between these elements and pH, CEC, TOC, sand, clay, oxides from secondary minerals, and the chemical index of alteration (CIA) for each basin.

Material and methods

Study area and sampling

The study sampling was performed in six profiles in the Cerrado sandy soils at the Parnaíba–São Francisco Basin transition in the northeast of Brazil (Fig. 1). According to the Köppen's climate classification map for Brazil (Alvares et al., 2013), the climate is Aw, defined as a humid tropical climate with a rainy season in the summer and a dry season in the winter. The annual average rainfall and temperature ranges are 900–1200 mm and 18–36 °C, respectively.

All the studied soil profiles were dug in areas under minimum anthropogenic influence. The sampling sites were selected based on their ability to represent different soil classes and parent materials at the studied scale, as described by Pfaltzgraff (2010). Profiles 1 (P1), 2 (P2), and 3 (P3) represent the Parnaíba Basin soils, whereas Profiles 4 (P4), 5 (P5), and 6 (P6) represent the São Francisco Basin soils. They were derived from Paleo-Mesozoic sedimentary materials, mainly represented by sandstones of different origins (Fig. 1). P1, P2, and P3 soils were formed from Carboniferous to Permian materials, while P4, P5, and P6 soils were formed from Cretaceous materials (Pfaltzgraff et al., 2010).
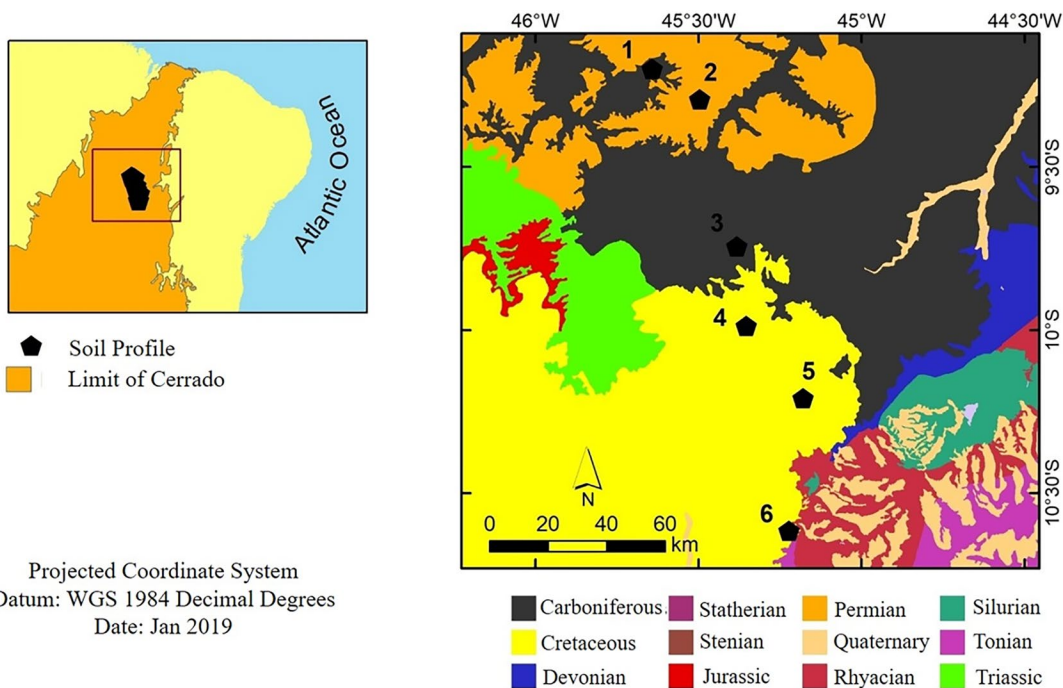
PARBAÍBA BASIN SOIL:

1. NEOSSOLO LITÓLICO Distrófico fragmentário[a]
    Lithic Udorthents[b]
    Piauí Formation, Balsas Group[c]

2. LATOSSOLO AMARELO Distrófico psamítico[a]
    Typic Haplustox[b]
    Pedra-de-Fogo Formation, Balsas Group[c]

3. CAMBISSOLO HÁPLICO Ta Eutrófico típico[a]
    Aridic Haplustept[b]
    Piauí Formation, Balsas Group[c]

SÃO FRANCISCO BASIN SOILS:

4. NEOSSOLO QUARTZARÊNICO Órtico latossólico[a]
    Ustic Quartzipsamment[b]
    Urucuia Group[c]

5. GLEISSOLO HÁPLICO Tb Eutrófico típico[a]
    Typic Haplorthel[b]
    Areado Group[c]

6. NEOSSOLO QUARTZARÊNICO Órtico latossólico[a]
    Ustic Quartzipsamment[b]
    Urucuia Group[c]

Fig. 1 Soil profile location followed by their classification; [a]SiBCS, Brazilian Soil Classification System (Santos et al., 2018); [b]USDA, Keys to Soil Taxonomy (Soil Survey Staff, 2014); [c]Stratigraphy information of the sediment for each soil profile (adapted from Pfaltzgraff et al., 2010)

Vieira and Scherer (2017) report that in the region of the P1 location are found soils derived from sandstones formed by aeolian dune deposition, whereas in the region of the P3 location are found soils derived from sandstones formed by shorefaces deposited earlier than the aeolian dunes that formed the P1 parent material. Both parent materials belong to Piauí Formation. Lima Filho (1991) affirms that in the region of the P2 location are found soils derived from the Pedra-de-fogo Formation composed predominantly of fine-to-coarse-grained sandstones. On the other hand, Oliveira et al. (2014) report that soils in the P4 and P6 locations are found soils derived from Late Cretaceous materials of the Areado Group, composed of thick layers of fluvial and aeolian sandstones, with interleaving siltstones and shale of the Urucuia Group. Additionally, Fragoso et al. (2011) indicate that in the region of the P5 location are found soils derived from materials of the Areado Group, composed of sandstones, siltstones, shale, and conglomerates of fluvial environments.

An inox knife was used to performing the soil sampling in all horizons. The recommendations provided by Santos et al. (2015) were adopted for the morphological description performing. Chemical and physical analyses were performed for all samples. Nevertheless, mineralogical analysis was carried out only on samples from topsoil horizons and subsurface diagnostic horizons (Fig. 1). Soil classification was conducted according to the Brazilian Soil Classification System (Santos et al., 2018) and Keys to Soil Taxonomy from the United States Department of Agriculture (Soil Survey Staff, 2014) (Fig. 1).

Chemical, grain size, and clay fraction oxide analysis

The soil samples were air-dried and sieved through a 2-mm mesh nylon sieve. The chemical analyses carried out were the pH in water, exchangeable K^+, Ca^{2+}, Mg^{2+}, Al^{3+}, and TOC (Teixeira et al., 2017). The results obtained from the sorptive complex were used to calculate the CEC. The pipette method determined the grain size using a 1 mol L^{-1} sodium hydroxide solution as a dispersant agent (Gee & Or, 2002). The concentrations of SiO_2, Al_2O_3, Fe_2O_3, and TiO_2 from soil clay fractions were determined from dried sieved soil samples using sulfuric acid (1:1) extraction solution, followed by determination of Al_2O_3, Fe_2O_3, and

TiO_2 on the extracts by atomic absorption spectrophotometry (Teixeira et al., 2017) and SiO_2 by colorimetry (Kilmer, 1965).

Mineralogical analysis

X-ray diffraction (XRD) analysis was performed on the dried sieved soil samples and clay fractions. A Shimadzu 6000 diffractometer fitted with a graphite monochromator set to select Cu Kα radiation (operated at 40 kV and 20 mA) was used. The measurement range was 5–70 (for dried sieved soil), 3–40 (for natural clay), and 3–35 (for the others) at °2θ intervals, with a step size of 0.02°2θ and a count time of 1.0. Before the analysis, the clay was subjected to the following standard treatments: organic matter elimination (using 30% H_2O_2) and iron oxide elimination using the dithionite-citrate-bicarbonate method (Mehra & Jackson, 2013), except for natural clay samples, which did not have their iron oxides excluded.

Clays were oriented on glass slides with the following standard treatments: Mg saturation ($MgCl_2^{-1}$ mol L^{-1}), K saturation (KCl^{-1} mol L^{-1}), and heat treatment of K-saturated samples for 3 h at 25 °C (K 25 °C), 110 °C (K 110 °C), 350 °C (K 350 °C), and 550 °C (K 550 °C) (Whittig & Allardice, 1986). Clay mineral identification was based on the criteria described by Brindley and Brown (1980), Jackson (1975), and Moore and Reynolds (1997).

Major element analysis and chemical index of alteration calculation

The total concentrations of SiO_2, Al_2O_3, Fe_2O_3, CaO, K_2O, Na_2O, TiO_2, and ZrO_2 were determined by X-ray fluorescence (XRF) spectrometry with wavelength energy dispersion (Rigaku ZSX mini II–WDXRF-3KW). The sample was prepared via a hydraulic press at 25 t, and the fire loss was determined at 1000 °C. The total concentrations of Al_2O_3, Na_2O, CaO, and K_2O were used to calculate the chemical alteration index (CIA) (Nesbitt & Young, 1982) (Eq. 1).

$$CIA = \frac{Al_2O_3}{Al_2O_3 + Na_2O + CaO + K_2O} 100 \quad (1)$$

Analyzing PTEs and REEs

The PTEs As, Ba, Cr, Ni, Pb, Cu, V, and Zn, as well as the REEs La, Ce, Pr, Nd, Sm, Eu, Gd, Tb, Dy, Ho, Er, Yb, and Lu were extracted following the EPA method 3051A (United States Environmental Protection Agency–USEPA, 1998). According to Alloway (2013), this method extracts elements that are likely to become available for medium- and long-term use. A portion of each sample (0.25 g) was digested in closed Teflon vessels with 9 mL of HNO_3 combined with 3 mL of HCl (high purity acids; Merck, PA) onto an automated microwave digestion system and elemental content determination was carried out by inductively coupled plasma optical emission spectrometry (ICP-OES). All ICP-OES analyses were performed in triplicates. For the analytical data quality assurance, use of calibration curves, curve recalibration, high purity acids, analysis of reagents blanks, and certified standard reference materials (SRM 2709, San Joaquin soil) of the National Institute of Standards and Technology (NIST, 2002) were followed. The detection limits for various PTEs were as follows: 10^{-4} mg kg^{-1} (As), $> 10^{-5}$ mg kg^{-1} (Cr, Ni, Cu, V, and Zn), and $> 10^{-6}$ mg kg^{-1} (Ba and Pb). The detection limit for all REEs was 10^{-6} mg kg^{-1}. The recovery rates of both PTEs and REEs obtained from the SRM 2709 sample rates ranged between 80 and 110%.

Rare earth element data were normalized as suggested by Henderson (1984), using upper continental crust (UCC) values as a reference (Taylor & McLennan, 1985). The light rare earth elements/ heavy rare earth elements (LREEs/HREEs) and $(La/Yb)_N$ ratios were used to quantify REE fractionation. Rare earth element normalized data were also used to obtain Ce anomalies $[(Ce/(La \times Pr)^{0.5}]$ (Ce/Ce*) calculated according to Compton et al. (2003). A value below 1 indicates depletion, while a value above 1 indicates enrichment compared to the UCC.

Data analysis

Pearson's correlation, descriptive statistics, and regression analyses were used in this study. Pearson's correlation was used to assess the association between PTEs and REEs with soil attributes such as pH, CEC, TOC, sand, clay, clay fraction oxides, and CIA. Linear regression analyses between the $(La/Yb)_N$ ratios, and *CIA* values were performed to evaluate the association between fractionation and weathering intensity.

Results

General characterization

The soil profiles P1, P2, and P3 showed pH values ranging from 3.4 to 5.4, while those of P4, P5, and P6 varied from 4.3 to 5.6 (Table 1). Considering the USDA classification (Soil Quality Indicators, 2011), the pH indicates that Parnaíba Basin soils as well as the São Francisco Basin soils fluctuate between extremely acidic (3.5–4.4) and moderately acidic (5.6–6.0). Both basins showed CEC values lower than 12.7 cmol$_c$ kg^{-1} (Table 1). The TOC content in soils showed low expressivity, ranging from 0.1 to 13 g kg^{-1} in the Parnaíba Basin and 0.1 to 4.9 g kg^{-1} in the São Francisco Basin (Table 1).

Considering the guidelines for soil texture description from the World Reference Base for Soil Resources (WRB) (2014), edited by a working group of the International Union of Soil Sciences (IUSS), the studied soil profiles were distinguished as arenic and loamic textural qualifiers, with sand content higher than 65% and clay content less than 30% (Fig. 2). In the Parnaíba and São Francisco Basins, the mean concentration of sand decreased in the following order: P1 > P2 > P3 and P5 > P6 > P4 (Fig. 2). Profile 3 showed a higher clay content in the Parnaíba Basin soils, followed by P2 and P1 (Fig. 2). In the São Francisco Basin, P4 showed a higher mean clay fraction, followed by P6 and P1 (Fig. 2).

Oxides extracted from secondary minerals by sulfuric attack showed that in the Parnaíba Basin soils, Al_2O_3 is the oxide that occurs in a larger part of the secondary mineral structure. This was followed by SiO_2, Fe_2O_3, and TiO (Table 1). In the São Francisco Basin soils, Fe_2O_3 is the oxide that occurs in a larger part of the secondary mineral structure. This was followed by $SiO_2 = Al_2O_3$ and TiO_2 (Table 1).

Table 1 Characterization of general soil attributes and clay fraction oxides in samples from Brazilian sandy soils under Cerrado from Parnaíba–São Francisco Basin transition

Soil	Horizon	Depth	General soil attributes[a]			Oxides[b]			
		m	pH	CEC	TOC	SiO_2	Al_2O_3	Fe_2O_3	TiO_2
			H_2O	$cmol_c\ kg^{-1}$	$g\ kg^{-1}$				
Parnaíba Basin									
P1	A	0–0.1	5.2	3.1	2.0	12.8	13.7	6.0	1.5
	Cr	0.1–0.4	4.9	1.6	4.3	14.0	14.6	6.0	1.9
P2	A	0–0.1	4.7	1.2	0.1	16.0	51.1	8.0	1.7
	AB	0.1–0.25	5.1	1.0	0.1	23.0	46.5	6.0	2.0
	BA	0.25–0.45	3.4	1.8	0.1	37.4	56.3	26.0	4.5
	Bw1	0.45–1.2	3.9	5.9	5.5	28.8	67.2	18.0	3.6
	Bw2	1.2–1.8[+]	3.6	2.6	0.4	42.2	71.8	28.0	5.2
P3	A	0–0.1	3.4	1.8	0.1	38.0	39.8	24.0	4.4
	AB	0.1–0.2	3.6	1.6	0.1	32.0	45.9	22.0	4.5
	Bi	0.2–0.85	5.4	12.7	13.0	8.9	61.1	16.0	3.3
	BC	0.85–1.1	5.0	6.5	1.7	11.2	57.1	22.0	3.3
	Cr	1.1–1.3	4.6	10.5	11.0	25.6	53.0	34.0	8.3
São Francisco Basin									
P4	A1	0–0.2	4.3	6.3	4.9	29.6	11.8	22.0	7.3
	A2	0.2–0.55	4.6	4.3	3.1	34.0	20.4	42.0	9.4
	C1	0.55–1.13	4.7	3.6	1.3	16.1	24.4	56.0	11.8
	C2	1.13–2.0[+]	4.8	2.5	0.1	34.2	27.3	56.0	11.5
P5	A	0–0.17	5.6	4.8	4.7	15.1	13.0	10.0	3.4
	AE	0.17–0.36	5.4	2.7	0.7	11.8	11.4	8.0	3.4
	E	0.36–0.84	5.3	1.8	1.2	9.3	9.4	12.0	3.8
	EB	0.84–1.28	5.5	1.8	0.1	9.9	9.8	12.0	2.9
	Bg	1.28–1.68	5.4	2.9	0.1	15.0	22.4	14.0	3.7
P6	A1	0–0.3	5.6	3.6	2.7	14.0	16.8	8.0	2.4
	C1	0.3–0.6	5.4	2.3	0.7	14.3	21.0	8.0	2.4
	C2	0.6–1.1	5.3	2.0	0.7	15.1	23.9	8.0	2.9
	C3	1.1–2.0[+]	5.1	1.6	0.1	18.7	30.6	8.0	3.3

CEC cation exchange capacity, *TOC* total organic carbon

[a]pH, hydrogen ion concentration

[b]SiO_2, Al_2O_3, Fe_2O_3, and TiO_2, and concentration of clay fraction oxides by the sulfuric attack

Soil mineralogy

The diffractograms obtained in non-oriented samples showed expressive peaks in the position of 0.33 nm in soil profiles P1, P2, and P3 (Fig. 3). The Parnaíba Basin soil profiles also presented peaks in the positions of 0.42, 0.24, 0.22, 0.21, 0.19, 0.18, and 0.16 nm (Fig. 3). However, the peaks in the positions of 0.71 and 0.35 nm observed in the profiles P2 and P3 were absent in the horizon A of P1 (Fig. 3). On the other hand, the peak in position 0.25 nm was observed only in the horizon A of P3. The São Francisco Basin soil profiles also have in common the presence of peaks in the positions of 0.42, 0.33, 0.24, 0.22, 0.21, 0.19, 0.18, and 0.16 nm, with higher expressivity in the position

of 0.33 nm (Fig. 3). In other words, it is possible to affirm that the diffractograms obtained in non-oriented samples showed the presence of quartz, feldspar, mica, and kaolinite in all studied soil profiles.

The diffractograms of the clay fractions are shown in Fig. 4. In the Parnaíba Basin soil profiles, peaks were presented in the positions of 0.71 and 0.33 nm after Mg- and K-saturation treatments followed by heat treatment at 25 °C, 110 °C, and 350 °C. However, the peaks disappeared after heat treatment at 550 °C. The P2 profile showed only two peaks of 0.71 and 0.33 nm. However, the horizon A of P1 presented peaks in the positions of 0.99, 0.42, and 0.33 nm even after heat treatment at 550 °C. The horizons A and Bi of P3 showed a peak in the position of 0.33 nm, easily observed even after
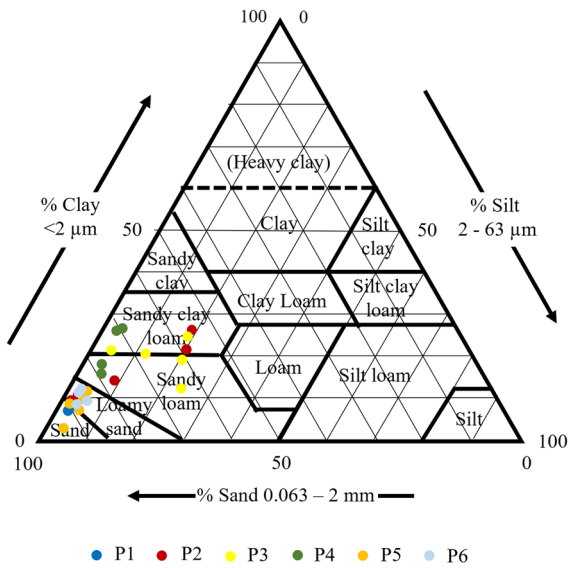
Fig. 2 Triangular diagram showing the texture distribution of the studied soils, according to IUSS Working Group WRB, World Reference Base for Soil Resources (2014)

heat treatment at 550 °C. The São Francisco Basin soil profiles also showed peaks in the positions of 0.71 and 0.33 nm after Mg- and K-saturation treatments followed by heat treatment at 25 °C, 110 °C, and 350 °C. These peaks were, however, destroyed after treatment at

550 °C. The horizons A of P4, Bg of P5, and A1 of P6 presented peaks in the positions of 0.99 nm and 0.33 nm, observed even after heat treatment at 550 °C, whereas the peak of 0.99 nm is absent and that of 0.33 nm is present in the horizon A of P5. Thus, the diffractograms of the clay fractions suggested that P1 and P3 have kaolinite and illite, whereas P2 only has kaolinite. On the other hand, P4, P5, and P6 have kaolinite and illite.

Major elements and chemical index of alteration

As expected, SiO_2 was the predominant oxide in the soil samples. In the Parnaíba Basin, the SiO_2 values ranged from 52.5 to 80.7%, whereas in the São Francisco Basin, it ranged from 80.5 to 90.6%. In general, the second most abundant oxide in the Parnaíba Basin is Fe_2O_3 (6.6 to 26.1%), followed by Al_2O_3 (5.1 to 15.4%), whereas in the São Francisco Basin, the amount of Al_2O_3 (3.6 to 12.2%) was higher than that of Fe_2O_3 (1.7 to 4.2%). Less than 1% CaO was found, except in the P1 topsoil. Profiles 2 and 3 showed K_2O values smaller than 1% and that of P4 (São Francisco Basin). All soil samples showed ZrO_2 values < 1%. In the Parnaíba Basin, the *CIA* values of P2 and P3 (Table 2) were between 93 and 99%, whereas those for P1 ranged from 47 to 52%. On the other hand, in the São Francisco Basin, P4

Fig. 3 X-ray diffractograms of soil samples from Brazilian sandy soils under Cerrado from Parnaíba–São Francisco Basin transition. Hz, horizon; P, profile; Fd, feldspar; Qz, quartz; Mc, mica; Kt, kaolinite
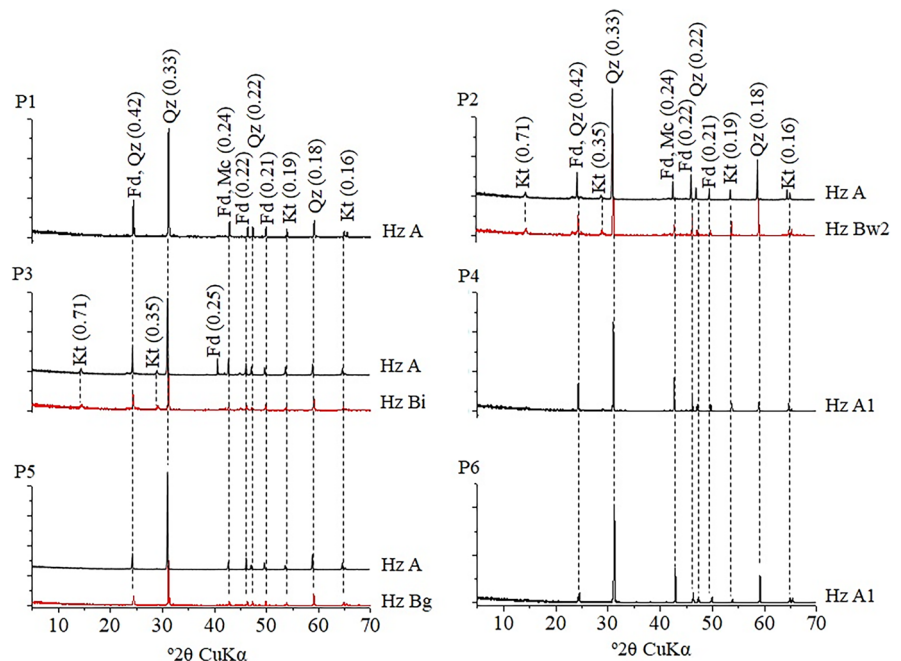
Fig. 4 X-ray diffractograms of clay fraction samples from Brazilian sandy soils under Cerrado from Parnaíba–São Francisco Basin transition. Hz, horizon; P, profile; Il, illite; Kt, kaolinite
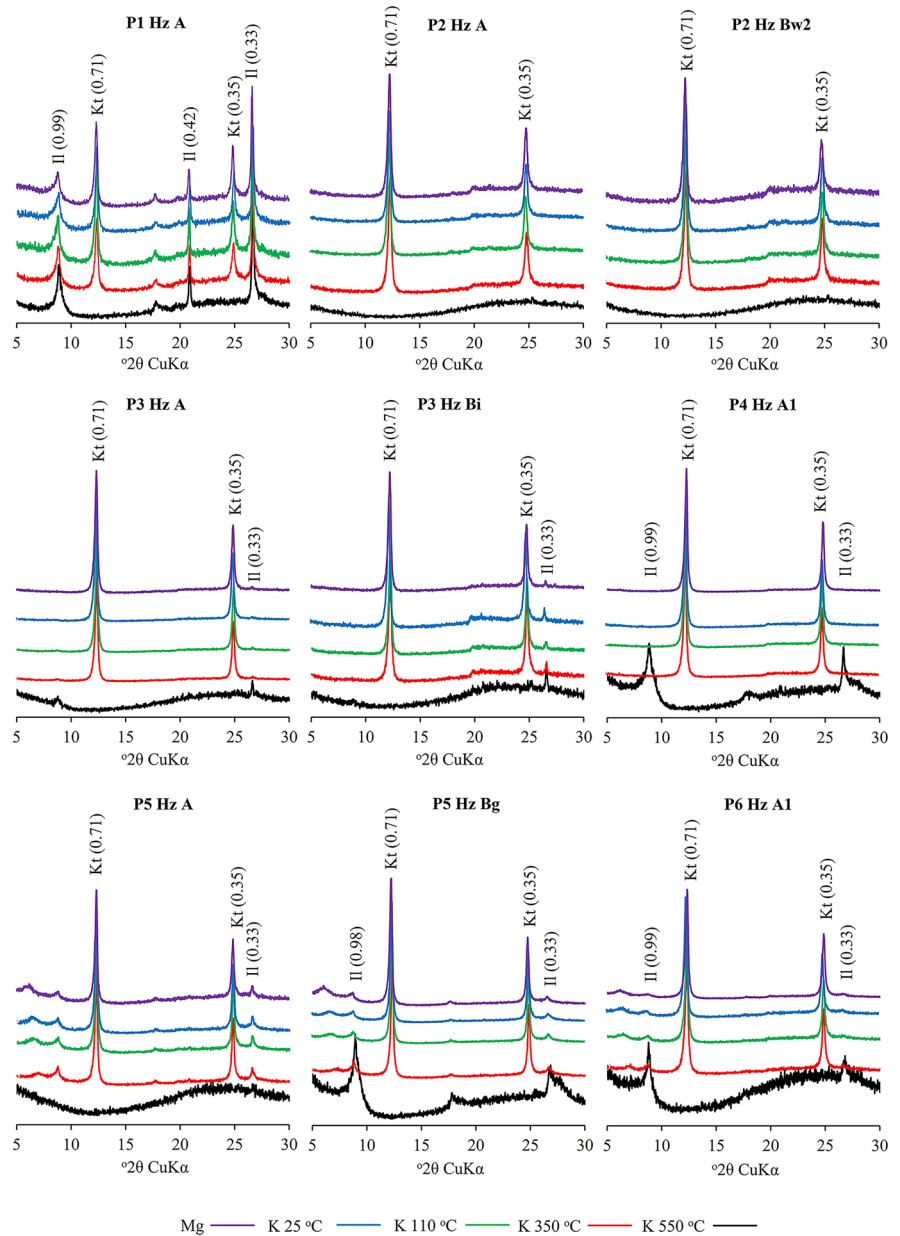
showed the highest *CIA* values (94–98%), followed by P6 (76–88%) and P5 (64–74%).

Background concentrations of PTEs and REEs in Parnaíba Basin soils

The concentrations of PTEs and REEs found in soils from the Parnaíba–São Francisco Basin transition are generally smaller than those observed in the Brazilian

state of Rio Grande do Norte and Sweden, as well as also in the upper continental crust (Table 3). The sum of the averages of REEs (ΣREEs) was equal to 40.5 mg kg^{-1} (Table 3). The mean background concentrations of PTEs were found to be in the following order: V > Ba > Cr > Pb > Zn > Cu > As > Ni. Profile 1 showed the highest background concentrations of As, Ba, Cu, Ni, and Zn. The elements Cr and V were found at higher concentrations in P2, whereas Pb was

Table 2 Major elements and chemical alteration index (CIA) from Brazilian sandy soils under Cerrado from Parnaíba and São Francisco Basins

Soil	Horizon	Depth	Major elements							CIA
		m	SiO_2	Al_2O_3	Fe_2O_3	CaO	K_2O	TiO_2	ZrO_2	
			g kg^{-1}							%
Parnaíba Basin										
P1	A	0 − 0.1	789	54	66	13	47	18	3	47
	CR	0.1 − 0.4	807	51	74	6	39	19	1	52
P2	A	0 − 0.1	717	98	145	3	0	34	3	97
	AB	0.1 − 0.25	664	127	167	0	1	38	3	99
	BA	0.25 − 0.45	631	128	196	3	0	37	5	97
	Bw1	0.45 − 1.2	564	154	220	3	0	43	5	98
	Bw2	1.2 − 1.8$^+$	525	149	261	2	1	51	6	99
P3	A	0 − 0.1	733	131	102	3	6	19	1	93
	AB	0.1 − 0.2	686	123	150	4	6	25	2	93
	Bi	0.2 − 0.85	672	135	150	3	4	30	3	95
	BC	0.85 − 1.1	676	145	146	3	6	22	2	94
	CR	1.1 − 1.3	663	141	160	2	8	23	3	93
São Francisco Basin										
P4	A1	0 − 0.2	881	65	21	4	0	21	1	94
	A2	0.2 − 0.55	852	82	37	0	1	21	2	98
	C1	0.55 − 1.13	854	90	36	4	0	15	1	96
	C2	1.13 − 2.0$^+$	805	122	42	4	2	16	2	96
P5	A	0 − 0.17	883	57	21	9	17	12	1	69
	AE	0.17 − 0.36	874	55	20	6	16	20	2	72
	E	0.36 − 0.84	891	52	17	5	15	19	1	72
	EB	0.84 − 1.28	906	36	19	5	15	16	2	64
	Bg	1.28 − 1.68	850	66	28	3	19	23	2	74
P6	A1	0 − 0.3	856	68	20	8	14	19	2	76
	C1	0.3 − 0.6	861	83	22	0	12	20	2	88
	C2	0.6 − 1.1	814	105	17	6	11	17	2	86
	C3	1.1 − 2.0$^+$	817	111	29	4	12	24	2	87

more abundant in P3 (Fig. 5). The mean background concentrations of REEs decreased in the following order: Ce > Nd > La > Pr > Gd > Sm > Dy > Tb = Yb > Eu > Er > Ho = Lu, which means that LREEs comprise 90% of the REEs, whereas HREEs comprise 10% (Table 3). Among the three studied Parnaíba Basin soils, only P3 had a $(La/Yb)_N$ ratio > 1 (Fig. 5). However, no correlation was observed between the $(La/Yb)_N$ ratio and CIA values ($R^2 = 0.47$, $P = 0.83$). The Ce/Ce* ratio ranged from 0.2 to 0.4, indicating a negative Ce anomaly in soils from the Parnaíba Basin (Fig. 5).

Background concentrations of PTEs and REEs in São Francisco Basin soils

The ΣREEs was equal to 35.3 mg kg^{-1} (Table 3), in other words, both smaller than found in soils from Parnaíba Basin. The mean background concentrations of PTEs in soils from the São Francisco Basin decreased in the following order: Ba > V > Cr > Pb > Zn > Cu > Ni (Fig. 5). All samples from that basin showed values of As below the detection limit (Table 3). Profile 6 had the highest concentration of all PTEs studied, followed

Table 3 Means of potentially toxic elements (PTEs) and rare earth elements (REEs) in Brazilian sandy soils under Cerrado from Parnaíba Basin, São Francisco Basin, Brazil, Sweden, and upper continental crust (UCC)

mg kg^{-1}		Parnaíba Basin					São Francisco Basin					RN-Brazil[a,b]	Sweden[c]	UCC[d]
		BDL	Mean	StDev	Min	Max	BDL	Mean	StDev	Min	Max	Mean	Mean	Mean
PTEs	As	3	2.5	1.2	1.5	5.4	13	-	-	-	-	0.9	2.5	1.50
	Ba	1	27.6	30.1	1.0	94.64	0	17.4	12.2	1.8	33.7	58.9	32.0	630.0
	Cr	0	20.2	11.6	6.4	38.15	0	3.9	1.8	1.8	7.2	30.9	8.1	35.0
	Ni	0	2.2	1.0	1.3	4.703	0	0.9	0.6	0.3	1.8	19.8	6.7	20.0
	Pb	0	5.7	5.0	0.7	14.28	0	2.8	1.5	1.0	5.9	16.2	24.1	20.0
	Cu	8	3.0	3.3	0.1	6.85	4	1.6	1.5	0.1	4.2	13.7	5.0	25.0
	V	0	35.8	13.7	20.9	61.37	0	4.2	1.0	3.0	5.8	-	32.1	60.0
	Zn	1	3.0	3.5	1.2	12.9	4	2.5	1.1	0.8	4.3	23.8	7.0	71.0
REEs	La	0	7.1	6.0	1.0	15.6	0	5.4	4.4	1.9	13.8	18.9	13.9	30.0
	Ce	0	17.9	10.1	6.7	34.1	0	14.0	13.2	3.5	37.3	40.4	28.0	64.0
	Pr	0	1.8	1.4	0.4	4.3	9	1.5	0.7	0.4	2.3	7.3	3.3	7.1
	Nd	0	8.2	6.5	2.0	19.9	0	5.5	5.3	1.4	15.7	15.8	24.0	26.0
	Sm	1	1.0	0.5	0.2	2.0	9	1.9	0.5	1.1	2.3	3.0	2.3	4.5
	Eu	5	0.5	0.3	0.1	0.8	3	0.4	0.4	0.0	1.1	0.5	0.5	0.9
	Gd	1	1.4	0.9	0.5	3.1	9	2.8	0.6	2.0	3.4	2.6	2.4	3.8
	Tb	2	0.5	0.1	0.3	0.6	10	0.5	0.0	0.4	0.5	0.5	0.3	0.6
	Dy	3	0.8	0.5	0.1	1.4	1	1.0	1.2	0.2	3.1	1.0	1.9	3.5
	Ho	10	0.3	0.1	0.3	0.3	7	0.5	0.2	0.2	0.8	0.3	0.4	0.8
	Er	9	0.4	0.0	0.4	0.4	9	1.2	0.3	0.9	1.4	0.7	1.2	2.3
	Yb	0	0.5	0.1	0.4	0.7	0	0.4	0.4	0.1	1.2	0.6	1.2	2.2
	Lu	0	0.3	0.1	0.2	0.5	7	0.1	0.1	0.1	0.2	0.2	0.2	0.3
	ΣREEs		40.5					5.4	4.4	1.9	13.8	91.8	79.6	146.0

BDL number of samples below the detection limit, *StDev* standard deviation, *Min* minimum, *Max* maximum

[a]Preston et al. (2014)

[b]Silva et al. (2018)

[c]Tyler and Olsson (2002)

[d]Average upper continental crust fromTaylor and McLennan (1985)

by P5 and P4 (Fig. 5). The mean background concentrations of REEs decreased in the following order: Ce > Nd > La > Gd > Sm > Pr > Er < Dy < Tb = Ho < Eu = Yb > Lu, which means that LREEs embrace 82% of the REEs, whereas HREE embraces 18% (Table 3). Profiles 4 and 5 showed $(La/Yb)_N$ ratios > 1 (Fig. 5), but no correlation was observed between the $(La/Yb)_N$ ratio and *CIA* values ($R^2 = 0.02$, $P = 0.64$). The Ce/Ce* ratio ranged from 0.4 to 0.5, indicating a negative Ce anomaly in soils from the São Francisco basin (Fig. 5).

Correlation of PTEs and REEs with soil attributes at the Parnaíba Basin

Considering all the studied PTEs, only As, Ba, and Cu did not show any statistically significant correlation with the studied soil attributes in the Parnaíba Basin soils. A correlation was observed between clay and Cu (−0.97, $P < 0.05$). The CEC and Pb also showed a correlation (0.69, $P < 0.05$), as well as Al_2O_3 and Cr (0.66, $P < 0.05$) and V (0.71, $P < 0.05$), and *CIA* with Cr (0.59, $P < 0.05$). On the other hand,
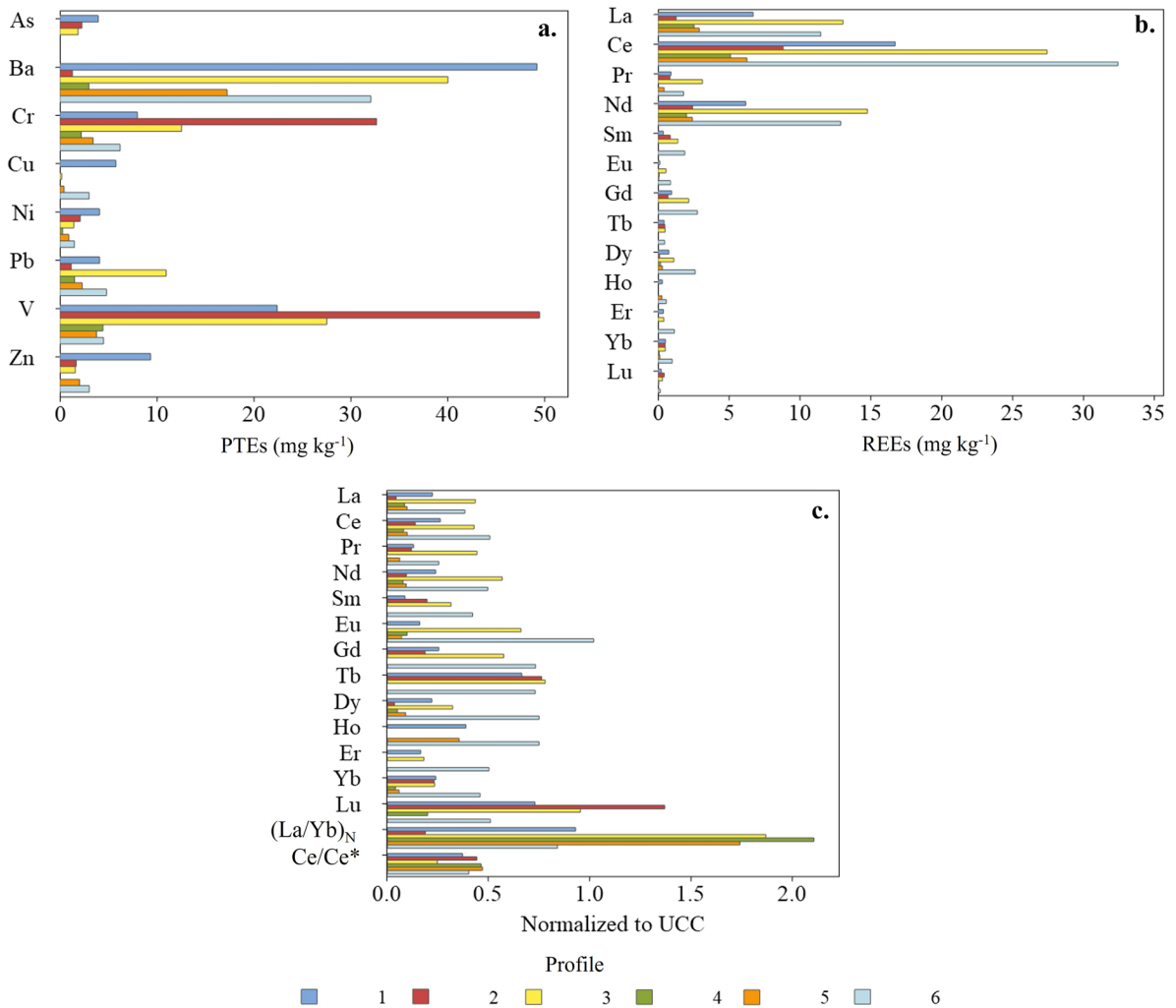
Fig. 5 a. Potentially toxic element concentrations and rare earth element concentrations (b., non-normalized data and c., normalized data)

a negative correlation was observed between Al_2O_3 and Ni (-0.71, $P < 0.05$) and Zn (-0.79, $P < 0.01$), whereas *CIA* was the same as Ni (-0.85, $P < 0.01$), Cu (-0.98, $P < 0.05$), and Zn (-0.90, $P < 0.01$).

Significant correlations were observed between La, Ce, Pr, Nd, Sm, Gd, Eu, and Tb with the studied soil attributes in the Parnaíba Basin soils. Clay showed a correlation with Sm (0.63, $P < 0.05$). A correlation was also observed between TOC and Pr (0.63, $P < 0.05$), Nd (0.61, $P < 0.05$), and Gd (0.70, $P < 0.05$). A correlation was observed between CEC and La (0.65, $P < 0.05$), Ce (0.66, $P < 0.05$), Pr (0.77, $P < 0.01$), Nd (0.72, $P < 0.05$), Sm (0.70, $P < 0.05$), and Gd (0.82, $P < 0.01$). Similarly, Al_2O_3 showed a positive correlation with Eu (0.80, $P < 0.05$) and Lu (0.78, $P < 0.01$), whereas Fe_2O_3 showed a positive correlation with Sm (0.84, $P < 0.01$) and Eu (0.83, $P < 0.05$). The TiO_2 showed a correlation with Pr (0.60, $P < 0.05$), Sm (0.87, $P = 0.00$), Eu (0.76, $P < 0.05$), and Tb (0.68, $P < 0.05$), whereas *CIA* showed a correlation with Eu (0.77, $P < 0.05$) and Lu (0.62, $P < 0.05$).

Correlation of PTEs and REEs with soil attributes at the São Francisco Basin

In São Francisco Basin soils, pH, clay, SiO_2, Al_2O_3, Fe_2O_3, TiO_2, and *CIA* showed statistically significant correlations with PTEs. The pH showed a correlation with Ba (0.71, $P < 0.05$) and Ni (0.59, $P < 0.05$), whereas clay was correlated with Ba (–0.61, $P < 0.05$) and Cu (0.67, $P < 0.05$). A correlation was also observed between SiO_2 and Cu (0.78, $P < 0.05$) and Zn (0.69, $P < 0.05$). On the other hand, Al_2O_3 was correlated with Cu (0.87, $P < 0.01$) and V (0.88, $P < 0.01$). The Fe_2O_3 showed a correlation with Ba (−0.78, $P < 0.01$), Cr (−0.58, $P < 0.05$), Ni (−0.71, $P < 0.05$), Cu (−0.68, $P < 0.05$), and Zn (−0.67, $P < 0.05$), whereas TiO_2 was correlated with Ba (−0.82, $P < 0.01$), Cr (−0.61, $P < 0.05$), Ni (−0.72, $P < 0.05$), and Pb (−0.58, $P < 0.05$). Chemical index of alteration was correlated with Cu (0.91, $P < 0.01$).

Among all the studied REEs, Ho and Lu proposed a statistically significant correlation with soil attributes. Sand was correlated with Lu (0.82, $P < 0.05$). The Al_2O_3 content was positively correlated with Ho (0.82, $P < 0.05$), and Fe_2O_3 showed a correlation with Ho (−0.82, $P < 0.05$) and Lu (−0.86, $P < 0.05$). In contrast, TiO_2 showed a correlation with Lu (−0.83, $P < 0.05$).

Discussions

As expected, the sedimentary nature of the soils formed in the Parnaíba and São Francisco Basins provided low concentrations of both PTEs and REEs. The low values of these metals recovered in soils derived from sedimentary rocks are associated with poor parent materials (mainly sandstones) and significant weathering because of the predominance of quartz in the sand fraction, as well as the reduced amount of clay. Moreover, kaolinite is the main phyllosilicate present in these soils, which does not offer an appreciable amount of negative charges at the low pH conditions prevailing in the Parnaíba and São Francisco Basin soils. This region is widely cultivated with soybean and other grains. Therefore, monitoring REEs and PTEs in these low buffer capacity agricultural soils is crucial to maintain food security and to avoid contamination of water resources due to metal leaching.

Despite the predominance of quartz, the presence of V in the Parnaíba Basin soils indicates that mafic rocks have influenced the parent materials of the soils. However, the concentration of V in soils from the Parnaíba Basin is smaller than that found in soils derived from mafic rocks, which may be seen as a typical characteristic of sandy soils of the Parnaíba Basin. According to Kabata-Pendias (2011), these values have a typical range of 100–250 mg kg^{-1}. The understanding that parent material that formed soils of the Parnaíba Basin influenced mafic rocks may also be used to justify why soils from the São Francisco Basin have approximately 66 mg kg^{-1} less PTEs than Parnaíba Basin soils. Considering that V displays various behaviors in response to its geochemical characteristics, the positive relation between V and Al_2O_3 may indicate isomorphic substitution of Al for V in clay structures or the adsorption of V by these minerals. According to Kabata-Pendias (2011), it is typical the replacement of Al by V in crystal structures. Zhu et al. (2018) reported that in soils of low pH, kaolinite may play an essential role in V adsorption, with a high adsorption capacity at pH between 4 and 10. The variation in V concentrations among Brazilian sandy soils under the Cerrado at the Parnaíba–São Francisco Basin transition also indicates that pedogenetic processes play an important role in the geochemistry of this metal in soils.

As observed in soils from the Parnaíba Basin, V is positively correlated with Al_2O_3 in soils from the São Francisco Basin. This correlation may be in response to the same phenomenon: the isomorphic substitution of Al for V in clay structures or the adsorption of V by those minerals (Zhu et al., 2018). Although the R^2 values were observed, this correlation was more substantial in soils from the São Francisco Basin than in the Parnaíba Basin. This difference may be in response to the pH. P4, P5, and P6 have a pH between 4 and 10, which provides a better V adsorption condition for kaolinite (Zhu et al., 2018). The higher concentration of Ba in soils from the São Francisco Basin is associated with the significant presence of K_2O in those soils, especially in P5 and P6. The presence of K_2O has a clear connection with the presence of feldspar, hence, associating the Ba content to the presence of this primary mineral. According to Kabata-Pendias (2011), this relation occurs in response to the similar ionic radii of Ba and K. However, the weathering of feldspar is not followed by the adsorption and

immobilization of Ba by clays or iron oxides, despite the common association between Ba and clay minerals (Cappuyns, 2018). Sverjensky (2006) reported that elements such as Be, Mg, Ca, Sr, and Ra are competitive with Ba for adsorption sites on iron oxides, which may explain the negative correlation between Ba and Fe_2O_3. Sajih et al. (2014) also reported weak adsorption of Ba in iron oxides. The possible presence of iron oxides such as titanomaghemite, which refers to cation-deficient spinels in the Fe^{3+}-rich field in the series Fe_3O_4–Fe_2TiO_4–$FeTiO_3$–γ-Fe_2O_3, is the reason why TiO_2 has the same or similar correlation as Fe_2O_3 with PTEs, given that Al and Ti are common substitutions at octahedral sheets (Giovannini et al., 2020).

In soils from the Parnaíba Basin, Cr and Ni exhibited different behaviors, considering their correlation with Cr, Al_2O_3, and *CIA*. The correlation between Cr and Al_2O_3 may be associated with two possibilities. Since the Parnaíba Basin soils have kaolinite in their composition, one possibility is the isomorphic substitution of Al^{3+} for Cr^{3+} during the crystallization of its phyllosilicate. This same substitution is possible in the crystallization of illite present in the P1 and P2. The second possibility is the sorption of Cr^{6+} in charges from these clay minerals, such as kaolinite and illite. These two possibilities may be considered because naturally occurring Cr compounds have principal valences of $+3$ (chromic) and $+6$ (chromate) (Chrysochoou et al., 2016), with the chromic form (less toxic and less soluble) able to replace Al^{3+}. Chromium was negatively correlated with Fe_2O_3 and TiO_2 in soils from the São Francisco Basin. This information suggests that the Cr form that occurs in soils from that basin is mostly Cr^{6+}, which tends to be less adsorbed by iron oxides (Rajput et al., 2016). In other words, the concentration of Cr decreased with the formation of hematite, goethite, or another iron oxide. In addition, the reduction of Cr^{6+} to Cr^{3+} in these soils is due to the oxidic environment and low organic matter content (Li et al., 2020), as is found in these soils.

The chromate form (highly toxic and highly soluble) is readily absorbed by clays and hydrous oxides (Gonzalez-Rodriguez & Fernandez-Marcos, 2021). On the other hand, the negative correlation between Ni and Al_2O_3 may have resulted from Ni leaching after the formation of kaolinite and illite. Besides, Ni is quickly mobilized during weathering

(Kabata-Pendias, 2011) and kaolinite or illite does not adsorb Ni significantly in soils with acid pH (Savignan et al., 2021). Because the oxides from secondary minerals are also added in the *CIA* calculation, this explains its correlation with PTEs, which also correlate with Al_2O_3 or other oxides. Geochemically, Ni usually joins metallic Fe wherever such a phase occurs and is also associated with carbonates and ferromagnesian minerals (Kabata-Pendias, 2011). The positive correlation between Ni and pH in soils from the São Francisco Basin reflects an association between Ni and K_2O. This association occurs because K_2O has been observed in greater amounts in P5 and P6, which suggests higher content of feldspar in these soils as compared to P4. Regardless of the clay minerals and iron oxides being known by their efficiency in the Ni adsorption processes (Savignan et al., 2021), the negative correlation between Ni and Al_2O_3, and TiO_2 indicates that soil pH precludes this phenomenon. According to Mellis et al. (2017), the pool of variable charges that could work on Ni adsorption only appears at pH values above 6.5. It is important to mention that kaolinite is the primary phyllosilicate found in these clays, which strengthens this observation. Perhaps for the same reason, Pb is also negatively related to TiO_2.

The correlation between Pb and CEC indicates that charges provided by kaolinite, illite, and organic matter are involved in Pb adsorption processes. According to Kabata-Pendias (2011), weathering provides oxidation of Pb sulfides, enabling the incorporation of Pb in clay minerals, Fe and Mn oxides, and organic matter. In addition, Pb has weak solubility and can replace K, Ba, Sr, and Ca in minerals, and organic matter (Kabata-Pendias, 2011). Thus, the dynamics of Pb in soils may explain its correlation with CEC.

The positive correlation between Cu and clay, SiO_2, and Al_2O_3 is possibly due to the high affinity of Cu adsorbed by kaolinites and illites. According to Kabata-Pendias (2011), the clay fraction is the soil attribute with a larger capacity to explain the presence of Cu. Silicon dioxide and Al_2O_3 are present in illite and kaolinite crystals found in soils from the São Francisco Basin, and they may play this role. Nevertheless, the pH of these soils does not allow an increase in variable charges provided by iron oxides (Vindedahl et al., 2016), reflecting the low level of Cu adsorption by these oxides, resulting in a negative correlation between Cu and Fe_2O_3.

The soil pH controls Zn adsorption as well. This may explain the negative correlation between Zn and Al_2O_3 in soils from the São Francisco Basin. According to Hamidpour et al. (2019), the adsorption of Zn by clay minerals, especially kaolinite, may be minimal at pH below 5.5, which results in the easy mobilization and leaching of Zn. The positive correlation between Zn and SiO_2 is an indicative of the adsorption of Zn on the silica tetrahedron of kaolinites and illites in soils from the São Francisco Basin. Ferric oxide has not been efficient in such adsorption because of the negative correlation between this oxide and Zn. Although these soils have a pH below 6, the probable absence of competitive cations to adsorption sites on kaolinite edges may result in Zn adsorption on clay minerals, even with the presence of illite. The same behavior was reported by Hamidpour et al. (2019). According to Kabata-Pendias (2011), iron oxides appear to be of minor importance in Zn adsorption processes in sandy soils.

The absence of a statistically significant correlation between the (La/Yb)$_N$ ratio and the *CIA* indicates the low influence of climate on REE geochemistry in soils from the Parnaíba–São Francisco Basin transition and can be explained by the low REE concentrations in soils originated from sandstones. Soils derived from sandstones commonly exhibit lower fractionation among LREEs and HREEs than soils originated from igneous rocks (Landim et al., 2021; Pereira et al., 2019). The presence of (La/Yb)$_N$ ratios greater than 1 in the P3 (Parnaíba basin), P4, and P5 (São Francisco basin) reflects the influence of mafic material on the formation of these soils. This statement corroborates Bolarinwa and Bute (2016), who reported that magma evolution occurred through crystal fractionation, and the occurrence of this process may be recognized by observing (La/Yb)$_N$ ratios greater than 1. In addition, pedogenetic processes can fractionate and redistribute the REEs in the soils as a result of the weathering action.

According to the Oddo-Harkins rule, the REE content decreases with increasing atomic number (Laveuf & Cornu, 2009). The REEs of the higher background concentration were Ce, as found by Silva et al. (2018). The high Ce concentration in soils can be explained by the fact that Ce can occur in a Ce (IV) valence state and can be associated with the presence of Fe–Mn concretions. The negative Ce anomaly observed in this study may indicate a slight depletion of this element in soils from the Parnaíba–São Francisco Basin transition. Overall, the negative Ce anomalies also indicate the relative La and Pr enrichment in these soils. The variation in Ce anomalies in the Brazilian sandy soils under the Cerrado can be explained by the variability of the oxidation conditions. On the other hand, it may also indicate that UCC could not be the best choice to normalize data obtained in soils derived mainly from sandstones.

Rare earth elements are known to have similar geochemical properties (Laveuf & Cornu, 2009; Mihajlovic & Rinklebe, 2018). This statement may refer to the positive correlation of La, Ce, Pr, Nd, Sm, and Gd with CEC in soils from the Parnaíba Basin. The positive correlation among REEs suggests that these metals were likely released from the same primary minerals. The correlation between REEs and CEC is provided by forming complexes and chelates between organic materials and REEs (Davranche et al., 2015). However, this interpretation is more effective in observing that Pr, Nd, Sm, and Gd correlate with TOC. Soils with higher organic carbon concentrations often have greater REE enrichment than other soils (Tyler, 2004).

Even in sandy soils, there is relevance of charges provided sesquioxides from the clay fraction in the adsorption of REEs. The association of Pr, Sm, Eu, Tb, and Lu with some of these sesquioxides was observed in this study. Nevertheless, the isomorphic substitution of Al^{3+} for REEs is also a possibility. In other words, illite and kaolinite are responsible for explaining some of the REEs in soils from the Parnaíba Basin. Iron oxides are also important in these soils. According to Courtois (1974), iron oxides tend to expulse REEs during the crystallization process. However, in amorphous iron oxides, the presence of REEs is significant (Compton et al., 2003). This statement indicates that iron oxides or titano-iron oxides in Parnaíba Basin soils are probably amorphous or have low crystallinity, resulting in their association with Pr, Sm, Eu, and Tb. According to Laveuf and Cornu (2009), weathering commonly promotes REE depletion in soils under tropical conditions. In this study, this phenomenon is associated with Ho and Lu, considering that these two REEs have a positive correlation with CIA. However, in general, the lack of a significant correlation between most REEs, and *CIA* indicates a small effect of weathering intensity on REE depletion in soils from the Parnaíba Basin.

In contrast to what was observed in soils from the Parnaíba Basin, only Ho and Lu proposed a correlation with soil attributes in soils from the São Francisco Basin. As explained above, the three phenomena which may explain the positive correlation between Ho and Al_2O_3 are: (1) the adsorption of Ho by kaolinites, (2) the replacement of Al^{3+} in both illite and kaolinite, and (3) the presence of Ho in interlayer sites of illites. Similar results were also reported by Yan et al. (1999) and Coppin (2002). On the other hand, the negative correlation of Ho with Fe_2O_3 and Lu with Fe_2O_3 and TiO_2 may be in response to the crystallinity of iron oxides, which promotes such a correlation (Compton et al., 2003). This study demonstrates that the geochemistry of REEs vary between Brazilian sandy soils under the Cerrado at the Parnaíba–São Francisco Basin transition as a function of both parent material and weathering process. However, as reported by Temga et al. (2021), it is difficult to establish which factor among them is predominant, and the geochemical behavior of these metals may vary on a case-by-case basis.

Conclusions

The parent material governs the background concentrations of PTEs and REEs in Brazilian sandy soils under the Cerrado at the Parnaíba–São Francisco Basin transition. The background concentrations of these elements are low, but soils from the Parnaíba Basin have a generically higher concentration of PTEs than soils from the São Francisco Basin. The main factors governing the differences in the geochemistry of REEs and PTEs between Brazilian sandy soils under the Cerrado at the Parnaíba–São Francisco Basin transition are the parent material (mainly sandstones) and the weathering process.

In soils from the Parnaíba Basin, mainly Al_2O_3 has relevance in V and Cr geochemistry, as these elements increase with increasing Al_2O_3 content. On the other hand, the REEs have CEC as a soil attribute of higher relevance in the geochemistry of those elements in soils from the Parnaíba Basin, and this relevance divides the TOC, Fe_2O_3, and TiO_2 minerals from the clay fraction. In soils from the São Francisco Basin, the geochemistry of PTEs is possibly associated with kaolinite, especially Cu, V, and Zn. In contrast, the Ba concentration was associated with the presence of feldspar. Unlike soils from the Parnaíba

Basin, the REEs do not correlate with the studied soil attributes, except for Ho and Lu. Holmium had a positive association with Al_2O_3. Ho and Lu are negatively related to the presence of iron oxides.

Availability of data and material The data that support the findings of this study are available from the corresponding author upon reasonable request.

Declarations

Conflict of interest The authors declare no competing interests.

References

Alfaro, M. R., Montero, A., Ugarte, O. M. U., Nascimento, C. W. A., Accioly, A. M. A., Biondi, C. M., & Silva, Y. J. A. B. (2015). Background concentrations and reference values for heavy metals in soils of Cuba. *Environmental Monitoring and Assessment, 187*(1), 4198. https://doi.org/10.1007/s10661-014-4198-3

Alfaro, M. R., Nascimento, C. W. A., Biondi, C. M., Silva, Y. J. A. B., Silva, Y. J. A. B., Accioly, A. M. A., Montero, A., Ugarte, O. M., & Estevez, J. (2018). Rare-earth-element geochemistry in soils developed in different geological settings of Cuba. *CATENA, 162*, 317–324. https://doi.org/10.1016/j.catena.2017.10.031

Alloway, B. J. (2013). *Heavy metals in soils: Trace metals and metalloids in soils and their bioavailability*. Springer.

Alvares, A. A., Stape, J. L., Sentelhas, P. C., de Moraes Gonçalves, J. L., & Sparovek, G. (2013). Köppen's climate classification map for Brazil. *Meteorologische*

Zeitschrift, 22(6), 711–728. https://doi.org/10.1127/0941-2948/2013/0507

Beuchle, R., Grecchi, R. C., Shimabukuro, Y. E., Seliger, R., Eva, H. D., Sano, E., & Achard, F. (2015). Land cover changes in the Brazilian Cerrado and Caatinga biomes from 1990 to 2010 based on a systematic remote sensing sampling approach. *Applied Geography, 58*, 116–127. https://doi.org/10.1016/j.apgeog.2015.01.017

Bolarinwa, A. T., & Bute, S. I. (2016). Petrochemical and tectonogenesis of granitoids in the Wuyo-Gubrunde Horst, Northeastern Nigeria: Implication for uranium enrichment. *Natural Resources Research, 25*(2), 197–210. https://doi.org/10.1007/S11053-015-9279-7

Brindley, G. W., & Brown, G. (1980). Crystal structures of clays minerals and their X-ray identification. *Mineralogical Society of Great Britain and Ireland*. https://doi.org/10.1180/mono-5

Cappuyns, V. (2018). Barium (Ba) leaching from soils and certified reference materials. *Applied Geochemistry, 88*, 68–84. https://doi.org/10.1016/j.apgeochem.2017.05.002

Chrysochoou, M., Theologou, E., Bompoti, N., Dermatas, D., & Panagiotakis, I. (2016). Occurrence, origin and transformation processes of geogenic chromium in soils and sediments. *Current Pollution Reports, 2*(4), 224–235. https://doi.org/10.1007/s40726-016-0044-2

Compton, J. S., White, R. A., & Smith, M. (2003). Rare earth element behavior in soils and saltpan sediments of a semiarid granitic terrain in the Western Cape. *South Africa. Chemical Geology, 201*(3–4), 239–255. https://doi.org/10.1016/S0009-2541(03)00239-0

Coppin, F. (2002). Etude expérimentale de l'adsorption des lanthanides sur une kaoliniteet une montmorillonite à 25 °C. Thesis of the University Toulouse III.

Courtois, C. (1974). *Les terres rares dans quelques minerais de fer*. Thesis of the University ParisSud.

Davranche, M., Gruau, G., Dia, A., Marsac, R., Pedrot, M., & Pourret, O. (2015). Biogeochemical factors affecting rare earth element distribution in shallow wetland groundwater. *Aquatic Geochemistry, 21*(2–4), 197–215. https://doi.org/10.1007/s10498-014-9247-6

Fragoso, D. G. C., Uhlein, A., Sanglard, J. C. D., Suckau, G. L., Guerzoni, H. T. G., & Faria, P. H. (2011). Geologia dos grupos Bambuí, Areado e Mata da corda na folha Presidente Olegário (1:100.000), MG: Registro deposicional do Neoproterozóico ao Neocretáceo da Bacia do São Francisco. *Genomos* 19(1), 28–38. https://doi.org/10.18285/geonomos.v19i1.60

Gee, G. W., & Or, D. (2002). Particle-size analysis. In: J. H. Dane & C. G. Topp (Eds.), *Methods of soil analysis: Physical methods*, (3rd ed., pp. 255–293). Soil Science Society of America.

Giovannini, A., Mitchell, R. H., Neto, A. C. B., Moura, C. A. V., Pereira, V. P., & Porto, C. G. (2020). Mineralogy and geochemistry of the Morro dos Seis Lagos siderite carbonatite, Amazonas. *Brazil. Lithos, 360–361*, 105433. https://doi.org/10.1016/j.lithos.2020.105433

Gonzalez-Rodriguez, S., & Fernandez-Marcos, M. L. (2021). Sorption and desorption of vanadate, arsenate and chromate by two volcanic soils of Equatorial Africa. *Soil Systems, 5*(2), 22. https://doi.org/10.3390/soilsystems5020022

Hamidpour, M., Karamooz, M., Akhgar, A., Tajabadipour, A., & Furrer, G. (2019). Adsorption of cadmium and zinc onto micaceous minerals: Effect of siderophore desferrioxamine B. *Pedosphere, 29*(5), 590–597. https://doi.org/10.1016/S1002-0160(17)60384-9

Henderson, P. (1984). *Rare earth element geochemistry*. Elsevier.

IUSS Working Group WRB, World Reference Base for Soil Resources. (2014) Update 2015. *International soil classification system for naming soils and creating legends for soil maps*. World Soil Resources Reports No. 106. FAO, Rome.

Jackson, M. L. (1975). *Soil chemical analysis: Advanced course*. University ofWisconsin.

Kabata-Pendias, A. (2011). *Trace elements in soils and plants* (4th ed.). CRC Press. https://doi.org/10.1201/b10158

Kilmer, V. J. (1965). Silicon. In C. A. Black (Ed.), *Methods of soil analysis. Part 2. Chemical and microbiological properties* (1st ed., pp. 959–962). Americam Society of Agronomy.

Landim, J. S. P., Silva, Y. J. A. B., Nascimento, C. W. A., Silva, Y. J. A. B., Nascimento, R. C., Boechat, C. L., Silva, C. M. C. A. C., Olinda, R. A., Barbosa, R. S., Silva, T. S., Biondi, C. M., & Collins, A. L. (2021). Distribution of rare earth elements in soils of contrasting geological and pedological settings to support human health assessment and environmental policies. *Environmental Geochemistry and Health*. https://doi.org/10.1007/s10653-021-00993-0

Laveuf, C., & Cornu, S. (2009). A review on the potentiality of rare earth elements to trace pedogenetic processes. *Geoderma, 154*(1–2), 1–12. https://doi.org/10.1016/j.geoderma.2009.10.002

Li, M., Guo, X., Wei, Y., Liu, A., Lu, J., Niu, X., Ma, Y., Li, S., Shang, Z., & Liu, X. (2020). Adsorption mechanism and structure-performance relationship of chromium ions by biochar. *Water, Air, & Soil Pollution, 231*, 517. https://doi.org/10.1007/s11270-020-04875-6

Lima Filho, F. P. (1991). *Fácies e ambientes deposicionais da Formação Piauí (Pensilvaniano), Bacia do Parnaíba*. Dissertation, Universidade de São Paulo.

Marafon, G., Barbosa, R. S., Lacerda, J. J. J., Martins, V., Silva, J. D. F., & Costa, O. C., Jr. (2020). C and P pool restoration by a no-tillage system on Brazilian Cerrado Oxisol in Piauí State. *Environmental Monitoring and Assessment, 192*(4), 254. https://doi.org/10.1007/s10661-020-8221-6

Matos, M. Q., & Felfili, J. M. (2010). Florística, fitossociologia e diversidade da vegetação arbórea nas matas de galeria do Parque Nacional de Sete Cidades (PNSC), Piauí. *Brasil. Revista Acta Botânica Brasílica, 24*(2), 483–496. https://doi.org/10.1590/S0102-33062010000200019

Mehra, O. D., & Jackson, M. L. (2013). Iron oxide removal from soils and clays by a dithionite–citrate system buffered with sodium bicarbonate. In E. Ingerson (Ed.), *Clays and clay minerals: Proceedings of The Seventh National Conference on Clays and Clay Minerals* (pp. 317–327). Pergamon Press. https://doi.org/10.1016/B978-0-08-009235-5.50026-7

Mellis, E. V., Casagrande, J. G., & Soares, M. R. (2017). Nickel adsorption and desorption in an acric oxisol as a function of pH, ionic strength and incubation time.

Ciência e Agrotecnologia, 41(1), 32–41. https://doi.org/10.1590/1413-70542017411020116

Mihajlovic, J., & Rinklebe, J. (2018). Rare earth elements in German soils - A review. *Chemosphere, 205*, 514–523. https://doi.org/10.1016/j.chemosphere.2018.04.059

Mittermeier, R. A., Gil, R. P., Hoffman, M., Pilgrim, J., Brooks, T. M., Mittermeier, C. G., Lamoreux, J., & Fonseca G. A. B. (2005). *Hotspots revisited: Earth's biologically richest and most endangered terrestrial ecoregions*. Cemex.

Moore, D. M., & Reynolds, R. C. (1997). *Identification of mixed-layered clay minerals*. Oxford University Press.

Nascimento, C. W. A., Lima, L. H. V., Silva, F. L., Biondi, C. M., & Campos, M. C. C. (2018). Natural concentrations and reference values of heavy metals in sedimentary soils in the Brazilian Amazon. *Environmental Monitoring and Assessment, 190*(10), 606. https://doi.org/10.1007/s10661-018-6989-4

National Institute of Standards and Technology - NIST. Standard Reference Materials – SRM 2709, 2710 and 2711. Addendum Issue Date: 18 Jan. 2002.

Nesbitt, H. W., & Young, G. M. (1982). Early Proterozoic climates and plate motions inferred from major element chemistry of lutites. *Nature, 299*, 715–717. https://doi.org/10.1038/299715a0

Oliveira, F. S., Varajão, A. F. D. C., Varajão, C. A. C., Boulangé, B., & Soares, C. C. V. (2013). Mineralogical, micromorphological and geochemical evolution of the facies from the bauxite deposit of Barro Alto, Central Brazil. *CATENA, 105*, 29–39. https://doi.org/10.1016/j.catena.2013.01.004

Oliveira, G. J. G., Vasconcelos, M. A. R., Crósta, A. P., Reimold, W. U., Góes, A. M., & Kowitz, A. (2014). Shatter cones and planar deformation features confirm Santa Marta in Piauí State, Brazil, as an impact structure. *Meteoritics & Planetary Science, 49*(10), 1915–1928. https://doi.org/10.1111/maps.12368

Pereira, B. A., Silva, Y. J. A. B., Nascimento, C. W. A., Silva, Y. J. A. B., Nascimento, R. C., Boechat, C. L., Barbosa, R. S., & Singh, V. P. (2019). Watershed scale assessment of rare earth elements in soils derived from sedimentary rocks. *Environmental Monitoring and Assessment, 191*(8), 514. https://doi.org/10.1007/s10661-019-7658-y

Pfaltzgraff, P. A. S. (2010). *Geodiversidade do Estado do Piauí*. Companhia de Pesquisa de Recursos Minerais

Preston, W., Nascimento, C. W. A., Biondi, C. M., Souza Júnior, V. S., Silva, W. R., & Ferreira, H. A. (2014). Valores de referência de qualidade para metais pesados em solos do Rio Grande do Norte. *Revista Brasileira De Ciência Do Solo, 38*(3), 1028–1037. https://doi.org/10.1590/S0100-06832014000300035

Rajput, S., Pittman, C. U., Jr., & Mohan, D. (2016). Magnetic magnetite (Fe_3O_4) nanoparticle synthesis and applications for lead (Pb^{2+}) and chromium (Cr^{6+}) removal from water. *Journal of Colloid and Interface Science, 468*(15), 334–346. https://doi.org/10.1016/j.jcis.2015.12.008

Rodrigues, L. U., & Silva, R. R. (2020). Boron availability in building up fertility in Cerrado soil of Tocantins. *Communications in Soil Science and Plant Analysis, 51*(5), 595–603. https://doi.org/10.1080/00103624.2020.1729371

Rótolo, G. C., Montico, S., Francis, C. A., & Ulgiati, S. (2015). How land allocation and techology innovation affect the sustainability of agriculture in Argentina pampas: An expanded life cycle analysis? *Agricultural Systems, 141*, 79–93. https://doi.org/10.1016/j.agsy.2015.08.005

Sajih, M., Bryan, N. D., Livens, F. R., Vaughan, D. J., Descostes, M., Phrommavanh, V., Nos, J., & Morris, K. (2014). Adsorption of radium and barium on goethite and ferrihydrite: A kinetic and surface complexation modelling study. *Geochimica Et Cosmochimica Acta, 146*, 150–163. https://doi.org/10.1016/j.gca.2014.10.008

Santos, H. G., Jacomine, P. K. T., Anjos, L. H. C., Oliveira, V. A., Lumbreras, J. F., Coelho, M. R., Almeida, J. A., Araujo Filho, J. C., Oliveira, J. B., & Cunha, T. J. F. (2018). *Sistema brasileiro de classificação de solos*. Embrapa Solos

Santos, R. D., Santos, H. G., Ker, J. C., Anjos, L. H. C., & Shimizu, S. H. (2015). *Manual de descrição e coleta de solo no campo*. Sociedade Brasileira de Ciência do Solo

Savignan, L., Lee, A., Coynel, A., Jalabert, S., Faucher, S., Lespes, G., & Chéry, P. (2021). Spatial distribution of trace elements in the soils of south-western France and identification of natural and anthropogenic sources. *CATENA, 205*, 105446. https://doi.org/10.1016/j.catena.2021.105446

Silva, C. M. C. A. C., Barbosa, R. S., Nascimento, C. W. A., Silva, Y. J. A. B., & Silva, Y. J. A. B. (2018). Geochemistry and spatial variability of rare earth elements in soils under different geological and climate patterns of the Brazilian Northeast. *Revista Brasileira De Ciência Do Solo., 42*, e0170342. https://doi.org/10.1590/18069657rbcs20170342

Silva, C. M. C. A. C., Nascimento, R. C., Silva, Y. J. A. B., Barbosa, R. S., Silva, Y. J. A. B., Nascimento, C. W. A., & van Straaten, P. (2020). Combining geospatial analyses to optimize quality reference values of rare earth elements in soils. *Environmental Monitoring and Assessment, 192*(7), 452. https://doi.org/10.1007/s10661-020-08406-y

Silva, J. F., Farinas, M. R., Felfili, J. M., & Klink, C. A. (2006). Spatial heterogeneity, land use and conservation in the Cerrado region of Brazil. *Journal of Biogeography, 33*(3), 536–548. https://doi.org/10.1111/j.1365-2699.2005.01422.x

Soil Quality Indicators. (2011). *Soil pH*. USDA-Natural Resources Conservation Service.

Soil Survey Staff. (2014). *Keys to Soil Taxonomy*. USDA-Natural Resources Conservation Service.

Sverjensky, D. A. (2006). Prediction of the speciation of alkaline earths adsorbed on mineral surfaces in salt solutions. *Geochimica Et Cosmochimica Acta, 70*(10), 2427–2453. https://doi.org/10.1016/j.gca.2006.01.006

Taylor, S. R., & McLennan, S. M. (1985). *The continental crust: Its composition and evolution: An examination of the geochemical record preserved in sedimentary rocks*. Blackwell Scientific.

Teixeira, P. C., Donagema, G. K., Fontana, A., & Teixeira, W. G. (2017). Manual de métodos de análise de solos. Embrapa Solos

Temga, J. P., Sababa, E., Mamdem, L. E., Bijeck, M. L. N., Azinwi, P. T., Tehna, N., Zame, P. Z., Onana, V. L., Nguetnkam, J. P., Bitom, L. D., & Ndjigui, P. D. (2021). Rare earth elements in tropical soils, Cameroon soils (Central Africa). *Geoderma Regional, 25*, 00369. https://doi.org/10.1016/j.geodrs.2021.e00369

Tyler, G. (2004). Rare earth elements in soil and plant systems - A review. *Plant and Soil, 276*, 191–206. https://doi.org/10.1007/s11104-005-4888-2

Tyler, G., & Olsson, T. (2002). Conditions related to solubility of rare and minor elements in forest soils. *Journal of Plant Nutrition and Soil Science 165*(5), 594-601. https://doi.org/10.1002/1522-2624(200210)165:5<594::AIDJPLN594>3.0.CO;2-K

United States Environmental Protection Agency–USEPA. (1998). *Method 3051A: Microwave assisted acid digestion of sediments, sludges, soils, and oils. SW-846: Test methods for evaluation of solid waste physical and chemical methods*, Office of Solid Waste, US.

Vieira, L. V., & Scherer, C. M. S. (2017). Facies architecture and high resolution sequence stratigraphy of anaeolian, fluvial and shallow marine system in the Pennsylvanian Piauí Formation, Parnaíba Basin, Brazil. *Journal of South American Earth Sciences, 76*, 238–256. https://doi.org/10.1016/j.jsames.2017.03.009

Vindedahl, A. M., Strehlau, J. H., Arnold, W. A., & Lee Penn, R. (2016). Organic matter and iron oxide nanoparticles: Aggregation, interactions, and reactivity. *Environmental Science: Nano, 3*(3), 494–505. https://doi.org/10.1039/c5en00215j

Whittig, L. D., & Allardice, W. R. (1986). X-ray diffraction techniques. In A. Klute (Ed.), *Methods of soil analysis* (2nd ed., pp 331–362). Soil Science Society of America.

Yan, X.-P., Kerrich, R., & Hendry, M. J. (1999). Sequential leachates of multiple grain size fractions from a clay-rich till, Saskatchewan, Canada: Implications for controls on the rare earth element geochemistry of pore waters in an aquitard. *Chemical Geology, 158*(1–2), 53–79. https://doi.org/10.1016/S0009-2541(99)00011-X

Yost, J. L., & Hartemink, A. E. (2019). Chapter four - Soil organic carbon in sandy soils: A review. In D. L. Sparks (Ed.), *Advances in agronomy* (pp. 217–310). Academic Press. https://doi.org/10.1016/bs.agron.2019.07.004

Zhu, H., Xiao, X., Guo, Z., Han, X., Liang, Y., Zhang, Y., & Zhou, C. (2018). Adsorption of vanadium (V) on natural kaolinite and montmorillonite: Characteristics and mechanism. *Applied Clay Science, 161*, 310–316. https://doi.org/10.1016/j.clay.2018.04.035